NANO LETTERS

2006
Vol. 6, No. 11
2422−2426

Controlling Quantum Transport through a Single Molecule

David M. Cardamone,* Charles A. Stafford, and Sumit Mazumdar

Department of Physics, University of Arizona, 1118 E. 4th Street, Tucson, Arizona 85721

Received April 13, 2006; Revised Manuscript Received July 19, 2006

ABSTRACT

We investigate multiterminal quantum transport through single monocyclic aromatic annulene molecules, and their derivatives, using the nonequilibrium Green function approach within the self-consistent Hartree–Fock approximation. We propose a new device concept, the quantum interference effect transistor, that exploits perfect destructive interference stemming from molecular symmetry and controls current flow by introducing decoherence and/or elastic scattering that break the symmetry. This approach overcomes the fundamental problems of power dissipation and environmental sensitivity that beset nanoscale device proposals.

From the vacuum tube to the modern CMOS transistor, devices which control the flow of electrical current by modulating an electron energy barrier are ubiquitous in electronics. In this paradigm, switching the current by raising and lowering the barrier, which must have a height greater than k_BT, generates a commensurate amount of heat, necessitating incredible power dissipation at device densities approaching the atomic limit.[1] A possible alternative is to exploit the wave nature of the electron to control current flow on the nanoscale.[2−7] In traditional mesoscopic devices, interference of electron waves is typically tuned via the Aharanov−Bohm effect;[8] however, for nanoscale devices such as single molecules, this is impractical due to the enormous magnetic fields required to produce a phase shift of order 1 rad.[2] Similarly, a device based on an electrostatic phase shift[5] would in small molecules require voltages incompatible with structural stability. We propose a solution that exploits perfect destructive interference stemming from molecular symmetry and controls quantum transport by introducing decoherence[9] or elastic scattering[3] from a third lead.

As daunting as the fundamental problem of the switching mechanism is the practical problem of nanofabrication.[1] In this respect, single molecules have a distinct advantage over other types of nanostructures, in that large numbers of identical "devices" can be readily synthesized. Single-molecule devices with two leads have been fabricated by a number of techniques.[10] Our transistor requires a third terminal coupled locally to the molecule, capacitively or via tunneling (see Figure 1). To date, only global gating of single-molecule devices has been achieved,[10] although there has been significant progress recently toward a locally coupled third terminal.[11]

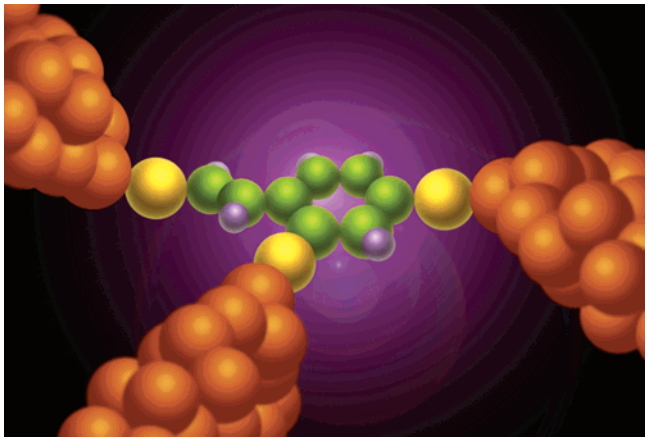

Figure 1. Artist's conception of a quantum interference effect transistor (QuIET). The colored spheres represent individual carbon (green), hydrogen (purple), and sulfur (yellow) atoms, while the three gold structures represent the metallic contacts. The vinyl linkage attached to the phenyl moiety can be replaced with alkene groups of arbitrary length (see text). A voltage applied to the leftmost contact regulates the flow of current between the other two. In addition to this structure (sulfonated vinylbenzene), full transport calculations were also carried out for structures in which the leftmost contact is connected to the benzene ring via alkene chains containing four and six carbon atoms.

This Letter reports the results of our recent theoretical investigations into the use of interference effects to create molecular transistors, leading to a new device concept, which we call the quantum interference effect transistor (QuIET). We demonstrate that for all monocyclic aromatic annulenes particular two-terminal configurations exist in which destruc-

* Corresponding author. Electronic mail: David_Cardamone@sfu.ca. Present address: Department of Physics, Simon Fraser University, BC V5A 1S6, Canada.

10.1021/nl0608442 CCC: $33.50
Published on Web 08/26/2006

tive interference blocks current flow and that transistor behavior can be achieved by supplying tunable decoherence or scattering at a third site. We also propose a realistic model for introducing scattering in a controllable way, using an alkene chain of arbitrary length (cf. Figure 1). Finally, we present nonequilibrium Green function (NEGF) calculations within the self-consistent Hartree−Fock approximation, indicating that the QuIET functions at room temperature with a current−voltage characteristic strikingly similar to macroscale transistors.

The Hamiltonian of the system can be written as the sum of three terms: $H = H_{\mathrm{mol}} + H_{\mathrm{leads}} + H_{\mathrm{tun}}$. The first is the π-electron molecular Hamiltonian

$$H_{\mathrm{mol}} = \sum_{n\sigma} \varepsilon_n d_{n\sigma}^{\dagger} d_{n\sigma} - \sum_{\langle nm\rangle\sigma} (t_{nm} d_{n\sigma}^{\dagger} d_{m\sigma} + \mathrm{H.c.}) + \sum_{nm} \frac{U_{nm}}{2} Q_n Q_m \quad (1)$$

where $d_{n\sigma}^{\dagger}$ creates an electron of spin σ in the π-orbital of the nth carbon atom, ε_n are the orbital energies, and $\langle\ \rangle$ indicates a sum over nearest neighbors. The tight-binding hopping matrix elements $t_{nm} = 2.2$, 2.6, or 2.4 eV for orbitals connected by a single bond, double bond, or within an aromatic ring, respectively. The final term of eq 1 contains intra- and intersite Coulomb interactions, as well as the electrostatic effects of the leads. The interaction energies are given by the Ohno parametrization[12,13]

$$U_{nm} = \frac{11.13\mathrm{eV}}{\sqrt{1 + 0.6117(R_{nm}/\text{Å})^2}} \quad (2)$$

where R_{nm} is the distance between orbitals n and m. $Q_n = \sum_{\sigma} d_{n\sigma}^{\dagger} d_{n\sigma} - \sum_{\alpha} C_{n\alpha} \mathrm{V}_{\alpha}/e - 1$ is an effective charge operator[14] for orbital n, where the second term represents a polarization charge. Here $C_{n\alpha}$ is the capacitance between orbital n and lead α, chosen consistent with the interaction energies of eq 2 and the geometry of the device, and V_{α} is the voltage on lead α. e is the magnitude of the electron charge.

Each metal lead α possesses a continuum of states, and their total Hamiltonian is

$$H_{\mathrm{leads}} = \sum_{\alpha=1}^{3} \sum_{k\in\alpha\sigma} \epsilon_k c_{k\sigma}^{\dagger} c_{k\sigma} \quad (3)$$

where ϵ_k are the energies of the single-particle levels in the leads, and $c_{k\sigma}^{\dagger}$ is an electron creation operator. Tunneling between molecule and leads is provided by the final term of the Hamiltonian

$$H_{\mathrm{tun}} = \sum_{\langle n\alpha\rangle} \sum_{k\in\alpha\sigma} (V_{nk} d_{n\sigma}^{\dagger} c_{k\sigma} + \mathrm{H.c.}) \quad (4)$$

where V_{nk} are the tunneling matrix elements from a level k within lead α to the nearby π-orbital n of the molecule. Coupling of the leads to the molecule via molecular chains, as may be desirable for fabrication purposes, can be included in the effective V_{nk}, as can the effect of substituents (e.g., thiol groups) used to bond the leads to the molecule.[15,16]

We use the NEGF approach[17,18] to describe transport in this open quantum system. The Green function of the full system is

$$G(E) = [E - H_{\mathrm{mol}} - \Sigma(E)]^{-1} \quad (5)$$

where Σ is an operator, known as the self-energy, describing the coupling of the molecule to the leads. The QuIET is intended for use at room temperature and operates in a voltage regime where there are no unpaired electrons in the molecule. Thus lead−lead and lead−molecule correlations, such as the Kondo effect, do not play an important role. Electron−electron interactions may therefore be included via the self-consistent Hartree−Fock method. H_{mol} is replaced by the corresponding mean-field Hartree−Fock Hamiltonian $H_{\mathrm{mol}}^{\mathrm{HF}}$, which is quadratic in electron creation and annihilation operators, and contains long-range hopping. Within mean-field theory, the self-energy is

$$\Sigma_{n\sigma,m\sigma'}(E) = -\frac{i}{2}\delta_{nm}\delta_{\sigma\sigma'} \sum_{\langle a\alpha\rangle} \Gamma_{\alpha}(E)\delta_{na} \quad (6)$$

where $\Gamma_{\alpha}(E) = 2\pi\sum_{k\in\alpha}|V_{nk}|^2\delta(E - \epsilon_k)$ is the Fermi Golden rule tunneling width. As a consequence, the molecular density of states changes from a discrete spectrum of delta functions to a continuous, width-broadened distribution. We take the broad-band limit,[17] treating Γ_{α} as constants characterizing the coupling of the leads to the molecule. Typical estimates[16] using the method of ref 19 yield $\Gamma_{\alpha} \lesssim 0.5$ eV, but values as large as 1 eV have been suggested.[15]

The effective hopping and orbital energies in $H_{\mathrm{mol}}^{\mathrm{HF}}$ depend on the equal-time correlation functions, which are found in the NEGF approach to be

$$\langle d_{n\sigma}^{\dagger} d_{m\sigma}\rangle = \sum_{\langle a\alpha\rangle} \frac{\Gamma_{\alpha}}{2\pi} \int_{-\infty}^{\infty} \mathrm{d}E\ G_{n\sigma,a\sigma}(E) G_{a\sigma,m\sigma}^{*}(E) f_{\alpha}(E) \quad (7)$$

where $f_{\alpha}(E) = \{1 + \exp[(E - \mu_{\alpha})/k_{\mathrm{B}}T]\}^{-1}$ is the Fermi function for lead α. Finally, the Green function is determined by iterating the self-consistent loop, eqs 5−7.

The current in lead α is given by the multiterminal current formula[20]

$$I_{\alpha} = \frac{2e}{h} \sum_{\beta=1}^{3} \int_{-\infty}^{\infty} \mathrm{d}E\ T_{\beta\alpha}(E)[f_{\beta}(E) - f_{\alpha}(E)] \quad (8)$$

where $T_{\beta\alpha}(E) = \Gamma_{\beta}\Gamma_{\alpha}|G_{ba}(E)|^2$ is the transmission probability[18] from lead α to lead β and a (b) is the orbital coupled to lead α (β). Similar mean-field NEGF calculations have been widely used to treat two-terminal transport through single molecules.[10]

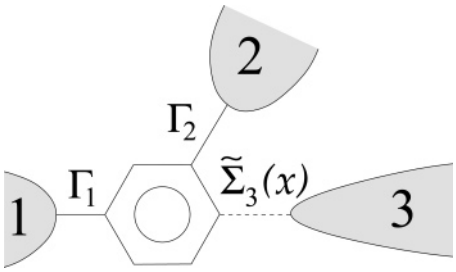

Figure 2. Schematic diagram of a QuIET based on benzene. Here Γ_1 and Γ_2 are the coupling strengths of metallic leads 1 and 2, connected in the meta orientation, to the corresponding π-orbitals of benzene. $\tilde{\Sigma}_3$, determined by a control variable x, is the retarded self-energy induced by lead 3. The real part of $\tilde{\Sigma}_3$ introduces elastic scattering, while the imaginary part introduces decoherence.

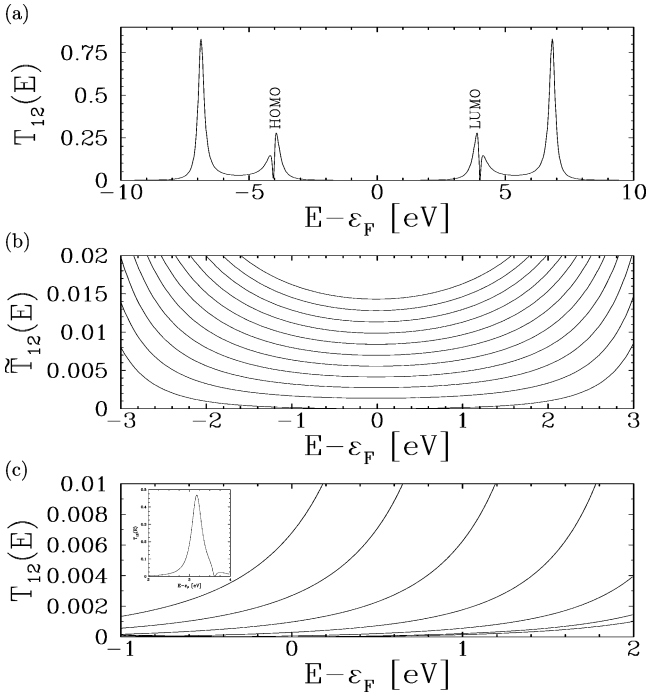

Figure 3. Effective transmission probability $\tilde{T}_{12}$ of the device shown in Figure 2, at room temperature, with $\Gamma_1 = 1.2$ eV and $\Gamma_2 = 0.48$ eV. Here ε_F is the Fermi level of the molecule. (a) $\tilde{\Sigma}_3 = 0$; (b) $\tilde{\Sigma}_3 = -i\Gamma_3/2$, where $\Gamma_3 = 0$ in the lowest curve, and increases by 0.24 eV in each successive one; (c) $\tilde{\Sigma}_3$ is given by eq 10 with a single resonance at $\varepsilon_\nu = \varepsilon_F + 4$ eV. Here $t_\nu = 0$ in the lowest curve and increases by 0.5 eV in each successive curve. Inset: Full vertical scale for $t_\nu = 1$ eV.

The QuIET exploits quantum interference stemming from the symmetry of monocyclic aromatic annulenes such as benzene. Quantum transport through single benzene molecules with two metallic leads connected at para positions has been the subject of extensive experimental and theoretical investigation;[10] however, a QuIET based on benzene requires the source (1) and drain (2) to be connected at meta positions, as illustrated in Figure 2. The transmission probability T_{12} of this device, for $\tilde{\Sigma}_3 = 0$, is shown in Figure 3a. Due to the molecular symmetry,[6] there is a node in $T_{12}(E)$, located midway between the HOMO and LUMO energy levels (see Figure 3b, lowest curve). This midgap node, at the Fermi level of the molecule, plays an essential role in the operation of the QuIET.

The existence of a transmission node for the meta connection can be understood in terms of the Feynman path integral formulation of quantum mechanics,[21] according to which an electron moving from lead 1 to lead 2 takes all possible paths within the molecule; observables relate only to the complex sum over paths. In the absence of a third lead ($\tilde{\Sigma}_3 = 0$), these paths all lie within the benzene ring. An electron entering the molecule at the Fermi level has de Broglie wavevector $k_F = \pi/2d$, where $d = 1.397$ Å is the intersite spacing of benzene (note that k_F is a purely geometrical quantity, which is unaltered by electron−electron interactions[22]). The two most direct paths through the ring have lengths $2d$ and $4d$, with a phase difference $k_F 2d = \pi$, so they interfere destructively. Similarly, all of the paths through the ring cancel exactly in a pairwise fashion, leading to a node in the transmission probability at $E = \varepsilon_F$.

This transmission node can be lifted by introducing decoherence or elastic scattering that break the molecular symmetry. Parts b and c of Figure 3 illustrate the effect of attaching a third lead to the molecule as shown in Figure 2, introducing a complex self-energy $\tilde{\Sigma}_3(E)$ on the π-orbital adjacent to that connected to lead 2. An imaginary self-energy $\tilde{\Sigma}_3 = -i\Gamma_3/2$ corresponds to coupling a third metallic lead directly to the benzene molecule. If the third lead functions as an infinite-impedance voltage probe, the effective two-terminal transmission is[9]

$$\tilde{T}_{12} = T_{12} + \frac{T_{13}T_{32}}{T_{13} + T_{32}} \tag{9}$$

The third lead introduces decoherence[9] and additional paths that are not canceled, thus allowing current to flow, as shown in Figure 3b. As a proof of principle, a QuIET could be constructed using a scanning tunneling microscope tip as the third lead, with tunneling coupling $\Gamma_3(x)$ to the appropriate π-orbital of the benzene ring, the control variable x being the piezovoltage controlling the tip−molecule distance.

By contrast, a real self-energy $\tilde{\Sigma}_3$ introduces elastic scattering, which can also break the molecular symmetry. This can be achieved by attaching a second molecule to the benzene ring, for example an alkene chain (cf. Figure 1). The retarded self-energy due to the presence of a second molecule is

$$\tilde{\Sigma}_3(E) = \sum_\nu \frac{|t_\nu|^2}{E - \varepsilon_\nu + i0^+} \tag{10}$$

where ε_ν is the energy of the νth molecular orbital of the second molecule, and t_ν is the hopping integral coupling this orbital with the indicated site of benzene. Figure 3c shows the transmission probability $T_{12}(E)$ in the vicinity of the Fermi energy of the molecule, for the case of a single side orbital at $\varepsilon_\nu = \varepsilon_F + 4$ eV. As the coupling t_ν is increased, the node in transmission at $E = \varepsilon_F$ is lifted due to scattering from the side orbital. The sidegroup introduces Fano antiresonances,[3,23] which suppress current through one arm of the annulene,

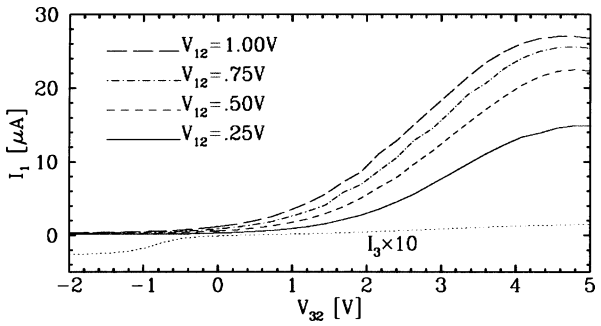

Figure 4. $I-V$ characteristic of the QuIET shown in Figure 1 at room temperature. The current in lead 1 is shown, where $V_{\alpha\beta} = V_\alpha - V_\beta$. Here, $\Gamma_1 = \Gamma_2 = 1$ eV. Γ_3 is taken as 0.0024 eV, which allows a small current in the third lead, so that the device amplifies current. A field-effect device with almost identical $I-V$ can be achieved by taking $\Gamma_3 = 0$. The curve for I_3 is for the case of 1.00 V bias voltage; I_3 for other biases looks similar.

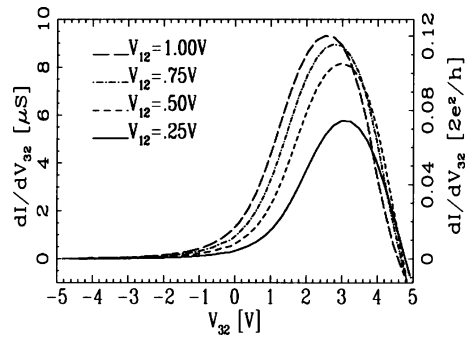

Figure 5. Transconductance dI/dV_{32} of the QuIET in Figure 1 with $\Gamma_3 = 0$. The characteristic is similar to a field-effect transistor, i.e., $I_3 = 0$ while $I_1 = -I_2 = I$. As in Figure 4, $\Gamma_1 = \Gamma_2 = 1$ eV, and the calculation was done for room temperature.

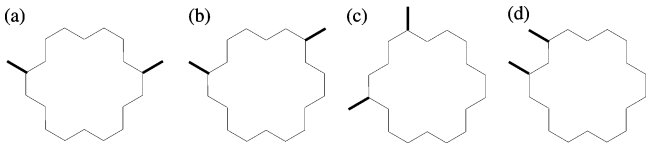

Figure 6. Source−drain lead configurations possible in a QuIET based on [18]-annulene. The bold lines represent the positioning of the two leads. Each of the four arrangements has a different phase difference associated with it: (a) π; (b) 3π; (c) 5π; and (d) 7π.

thus lifting the destructive interference. Put another way, the second molecule's orbitals hybridize with those of the annulene, and a state that connects leads 1 and 2 is created in the gap (see Figure 3c (inset)). In practice, either t_ν or ε_ν might be varied to control the strength of Fano scattering.

Tunable current suppression occurs over a broad energy range, as shown in Figure 3b; the QuIET functions with any metallic leads whose work function lies within the annulene gap. Fortunately, this is the case for many bulk metals, among them palladium, iridium, platinum, and gold.[24] Appropriately doped semiconductor electrodes[11] could also be used.

We show in Figure 4 the $I-V$ characteristic of a QuIET based on sulfonated vinylbenzene, whose molecular structure is given in Figure 1. The three metallic electrodes were taken as bulk gold, with $\Gamma_1 = \Gamma_2 = 1$ eV, while $\Gamma_3 = 0.0024$ eV, so that the coupling of the third electrode to the alkene sidegroup is primarily electrostatic. The device characteristic resembles that of a macroscopic transistor. As the voltage on lead 3 is increased, scattering from the antibonding orbital of the alkene sidegroup increases as it approaches the Fermi energies of leads 1 and 2, leading to a broad peak in the current. For $\Gamma_{1,2} \gg \Gamma_3 \neq 0$, the device amplifies the current in the third lead (dotted curve), emulating a bipolar junction transistor. Alkene chains containing four and six carbon atoms were also studied, yielding devices with characteristics similar to that shown in Figure 4, with the maximum current I_1 shifting to smaller values of V_{32} with increasing chain length. As evidence that the transistor behavior shown in Figure 4 is due to the tunable interference mechanism discussed above, we point out that if hopping between the benzene ring and the alkene sidegroup is set to zero, so that the coupling of the sidegroup to benzene is purely electrostatic, almost no current flows between leads 1 and 2.

For $\Gamma_3 = 0$, $I_3 = 0$ and the QuIET behaves as a field-effect transistor. The transconductance dI/dV_{32} of such a device is shown in Figure 5. For comparison, we note that an ideal single-electron transistor[25] with $\Gamma_1 = \Gamma_2 = 1$ eV has peak transconductance $(1/17)G_0$ at bias voltage 0.25 V and $(1/2)G_0$ at bias 1 V, where $G_0 = 2e^2/h$ is the conductance quantum. For low biases, the proposed QuIET thus has a higher transconductance than the prototypical nanoscale amplifier, while even for large biases its peak transconductance is comparable. Likewise, the load resistances required for a QuIET to have gain (load times transconductance) greater than 1 while in its "on" state are comparable to other nanoscale devices, $\sim 10/G_0$.

Operation of the QuIET does not depend sensitively on the magnitude of the lead−molecule coupling $\bar{\Gamma} = \Gamma_1\Gamma_2/(\Gamma_1 + \Gamma_2)$. The current through the device decreases with decreasing $\bar{\Gamma}$, but aside from that, the device characteristic was found to be qualitatively similar when $\bar{\Gamma}$ was varied over 1 order of magnitude. The QuIET is also insensitive to molecular vibrations: Only vibrational modes that simultaneously alter the carbon−carbon bond lengths and break the 6-fold symmetry within the benzene component can cause decoherence in a benzene "interferometer". Such modes are only excited at temperatures greater than about 500 K.

The QuIET mechanism applies to any monocyclic aromatic annulene with leads 1 and 2 positioned so the two most direct paths have a phase difference of π. Furthermore, larger molecules have other possible lead configurations, based on phase differences of 3π, 5π, etc. Figure 6 shows the lead configurations for a QuIET based on [18]-annulene.

The position of the third lead affects the degree to which destructive interference is suppressed. For benzene, the most effective location for the third lead is shown in Figures 1 and 2. It may also be placed at the site immediately between leads 1 and 2, but the transistor effect is somewhat reduced, since coupling to the charge carriers is less. The third, 3-fold symmetric configuration of leads completely decouples the third lead from electrons traveling between the first two leads.

For each monocyclic aromatic annulene, one 3-fold symmetric lead configuration exists, yielding no transistor behavior.

The QuIET's operating mechanism, tunable coherent current suppression, occurs over a broad energy range within the gap of each monocyclic aromatic annulene; it is thus a *very robust effect, insensitive to moderate fluctuations of the electrical environment of the molecule*. Although based on an entirely different, quantum mechanical, switching mechanism, the QuIET nonetheless reproduces the functionality of macroscopic transistors on the scale of a single molecule.

Acknowledgment. D.M.C. thanks G. Kirczenow for useful discussions. The authors thank Helen M. Giesel for creating the image used in Figure 1. This work was supported by National Science Foundation Grant Nos. PHY0210750, DMR0312028, DMR0406604, and PHY0244389.

References

(1) International Technology Roadmap for Semiconductors: 2004 Update. http://public.itrs.net.
(2) Sautet, P.; Joachim, C. *Chem. Phys. Lett.* **1988**, *153*, 511.
(3) Sols, F.; Macucci, M.; Ravaioli, U.; Hess, K. *Appl. Phys. Lett.* **1989**, *54*, 350.
(4) Joachim, C.; Gimzewski, J. K. *Chem. Phys. Lett.* **1997**, *265*, 353. Joachim, C.; Gimzewski, J. K.; Tang, H. *Phys. Rev. B* **1998**, *58*, 16407.
(5) Baer, R.; Neuhauser, D. *J. Am. Chem. Soc.* **2002**, *124*, 4200.
(6) Yaliraki, S. N.; Ratner, M. A. *Ann. N.Y. Acad. Sci.* **2002**, *960*, 153.
(7) Stadler, R.; Forshaw, M.; Joachim, C. *Nanotechnology* **2003**, *14*, 138.Stadler, R.; Ami, S.; Forshaw, M.; Joachim, C. *Nanotechnology* **2003**, *14*, 722.
(8) Washburn, S.; Webb, R. A. *Adv. Phys.* **1986**, *35*, 375.
(9) Büttiker, M. *IBM J. Res. Dev.* **1988**, *32*, 63.
(10) Nitzan, A.; Ratner, M. A. *Science (Washington, D.C.)* **2003**, *300*, 1384 and references therein.
(11) Piva, P. G.; DiLabio, G. A.; Pitters, J. L.; Zikovsky, J.; Rezeq, M.; Dogel, S.; Hofer, W. A.; Wolkow, R. A. *Nature (London)* **2005**, *435*, 658.
(12) Ohno, K. *Theor. Chim. Acta* **1964**, *2*, 219.
(13) Chandross, M.; Mazumdar, S.; Liess, M.; Lane, P. A.; Vardeny, Z. V.; Hamaguchi, M.; Yoshino, K. *Phys. Rev. B* **1997**, *55*, 1486.
(14) Stafford, C. A.; Kotlyar, R.; Das Sarma, S. *Phys. Rev. B* **1998**, *58*, 7091.
(15) Tian, W.; Datta, S.; Hong, S.; Reifenberger, R.; Henderson, J. I.; Kubiak, C. P. *J. Chem. Phys.* **1998**, *109*, 2874.
(16) Nitzan, A. *Annu. Rev. Phys. Chem.* **2001**, *52*, 681.
(17) Jauho, A.-P.; Wingreen, N. S.; Meir, Y. *Phys. Rev. B* **1994**, *50*, 5528.
(18) Datta, S. *Electronic Transport in Mesoscopic Systems*; Cambridge University Press: Cambridge, U.K., 1995; pp 293−342.
(19) Mujica, V.; Kemp, M.; Ratner, M. A. *J. Chem. Phys.* **1994**, *101*, 6849.
(20) Büttiker, M. *Phys. Rev. Lett.* **1986**, *57*, 1761.
(21) Feynman, R. P.; Hibbs, A. R. *Quantum Mechanics and Path Integrals*; McGraw-Hill: New York, 1965.
(22) Luttinger, J. M. *Phys. Rev.* **1960**, *119*, 1153.
(23) Clerk, A. A.; Waintal, X.; Brouwer, P. W. *Phys. Rev. Lett.* **2001**, *86*, 4636.
(24) Marder, M. P. *Condensed Matter Physics;* John Wiley & Sons: New York, 2000.
(25) Kastner, M. A. *Rev. Mod. Phys.* **1992**, *64*, 849.

NL0608442